journal

J. Am. Ceram. Soc., 94 [10] 3359–3363 (2011)
DOI: 10.1111/j.1551-2916.2011.04491.x

Structure and Optical Property of Polymer-Derived Amorphous Silicon Oxycarbides Obtained at Different Temperatures

Yiguang Wang,[*,‡] Kewei Wang,[‡] Ligong Zhang,[§] and Linan An[*,†,‡,¶]

[‡]National Key Laboratory of Thermostructure Composite, Northwestern Polytechnical University, Xi'an, Shaanxi 710072, China

[§]Laboratory of Excited State Process, Changchun Institute of Optics, Fine Mechanics and Physics, Chinese Academy of Science, Changchun 130032, China

[¶]Advanced Materials Processing and Analysis Center, University of Central Florida, Orlando, Florida 32816

Amorphous silicon carbides are prepared by pyrolysis of a polycarbosilane precursor at different temperatures between 1000° and 1400°C. The structures of the resultant materials are analyzed using X-ray diffraction, electron paramagnetic resonance, and Raman spectroscopy. The optical properties of the SiC ceramics are investigated by measuring their absorption spectra. It is found that there is a critical temperature range, at which the structural and optical behavior varied in different ways as a function of pyrolysis temperature. The evolution in structures is discussed and the optical behavior is explained in terms of the structural evolution during pyrolysis at different temperatures.

I. Introduction

Polymer-derived amorphous ceramics (PDCs) are a new class of multifunctional materials synthesized by thermal decomposition of polymeric precursors.[1] These materials possess many unique features compared with conventional ceramics. For example, PDCs possess a unique structure, which consists of an amorphous matrix and a randomly distributed self-assembled nanosized carbon cluster.[2] This unique structure correlates to many unusual material properties. Previous studies[3–5] have shown that the properties of PDCs strongly depend on the precursor chemistry and pyrolysis temperature. A detailed understanding of the property–structure relationships of PDCs can play a key role in further application and improvement of the materials. However, due to the complexity of the PDC structures, establishing such property–structure relationships is a huge challenge and cannot be achieved using only theoretical methods.

Optical/electronic behaviors of PDCs have received extensive attention due to their relevance for applications in electronic/optical devices.[6–10] Previously, the electronic structure of PDCs has been studied by measuring their optical absorption behavior.[11,12] Wang *et al.*[11] reported that polymer-derived amorphous silicon oxycarbonitrides (SiCONs) show two absorption mechanisms in different excitation energy regions. These authors also revealed that the band gaps of both transitions decrease with increasing pyrolysis temperature. However, these previous studies did not provide a detailed relationship between the optical behavior and the structures of these materials.

In this paper, we studied the structure and optical behavior of polymer-derived amorphous silicon oxycarbides (SiOC) obtained at different pyrolysis temperatures. The structure of the materials was investigated using X-ray diffraction (XRD), Raman, and electron paramagnetic resonance (EPR), and the optical behavior was studied by measuring their optical absorption. The optical behavior was discussed in terms of structural evolution.

II. Experimental Procedure

The SiOC ceramics studied here were synthesized by thermal decomposition of a liquid-phased polycarbosilane synthesized at Xiamen University. First the precursor was cured at 400°C for 2 h in an ultra-high-purity argon environment. The curing product was then ground to a powder and pressed into disks of 16 mm diameter and 1 mm thickness. Finally, the disks were pyrolyzed in a vertical furnace at temperatures ranging between 1000° and 1400°C for 4 h in flowing ultra-high-purity argon.

The thermal stability of the SiOC powder obtained at 900°C was investigated using a thermogravimetric analyzer (TGA, Netzsch STA 409 C/CD, Selb, Germany) in the temperature range of 900°–1400°C. The test was carried out under argon protection at a ramping rate of 10 K/min. The crystalline composition of the obtained materials was analyzed by XRD (Rigaku D/max-2400, Tokyo, Japan) using Cu$K\alpha$ radiation. Data were digitally recorded in a continuous scan mode in the angle (2θ) range of 20°–80° at a scanning rate of 0.12°/s. The free carbon phase in the ceramics was characterized using a Renishaw in-via Raman microscope (Renishaw, London, U.K.) with the 532 nm line of an Ar laser as the excitation source. The structural defects in these ceramics were studied by EPR at a frequency of 406.4 GHz.

The optical behavior of the ceramics was characterized by measuring their absorption spectra using a UV-3101 double-channel spectrometer (Shimadzu Co., Kyoto, Japan). The SiOC were first ground to a powder of $\sim$1 μm. The powder was then mixed with KBr and pressed into disks of 10 mm diameter and 0.5 mm thickness. The ratio of the SiOC to KBr was controlled so that the absorbance of the disks ranged between 0.2 and 0.8. The absorption spectra were obtained using a double-channel spectrometer. In order to remove the signal from KBr, two pure KBr disks of the same size were prepared. One was placed at a reference optical channel, and the other was placed at a sample channel to calibrate the base line. The absorption spectra of the KBr/SiOC samples were obtained by placing them at the sample channel. In this way, the absorption spectra of pure SiOC powder were obtained.

R. Riedel—contributing editor

Manuscript No. 28610. Received September 14, 2010; approved February 12, 2011.
This work was supported by the "111" program (B08040), the National Science Foundation of USA (DMR-0706526), and the National Natural Science Foundation of China (Grant No: 50972140).
*Member, The American Ceramic Society.
†Author to whom correspondence should be addressed. e-mail: lan@mial.ucf.edu

Table I. Composition of the Polymer-Derived Amorphous Silicon Carbides

Sample #	Pyrolysis temperature (°C)	Composition	Apparent formula
S1	1000	$SiC_{1.46}O_{0.06}$	$0.03SiO_2 \cdot 0.97SiC \cdot 0.49C$
S2	1100	$SiC_{1.45}O_{0.08}$	$0.04SiO_2 \cdot 0.96SiC \cdot 0.49C$
S3	1200	$SiC_{1.45}O_{0.07}$	$0.035SiO_2 \cdot 0.965SiC \cdot 0.485C$
S4	1250	$SiC_{1.43}O_{0.06}$	$0.03SiO_2 \cdot 0.97SiC \cdot 0.46C$
S5	1300	$SiC_{1.47}O_{0.06}$	$0.03SiO_2 \cdot 0.97SiC \cdot 0.50C$
S6	1400	$SiC_{1.46}O_{0.08}$	$0.04SiO_2 \cdot 0.96SiC \cdot 0.50C$

III. Results

The compositions of the ceramics obtained were measured using a combination of an IR carbon–sulfur analyzer and an oxygen–nitrogen analyzer.[13] The results are listed in Table I. It can be seen that the materials obtained at the different pyrolysis temperatures essentially have the same composition, suggesting that the materials are thermally stable (without further decomposition) in the testing temperature range. This is confirmed by the TGA result (Fig. 1), which reveals that there is no weight loss up to 1400°C for the sample obtained at 900°C. The results also reveal (from their apparent formula) that the materials contain a fairly large amount of extra carbon and a small amount of oxygen. Figure 2 shows the XRD patterns for the samples obtained at different pyrolysis temperatures. The XRD patterns for the samples pyrolyzed at temperatures between 1000° and 1200°C show no diffraction peaks, suggesting that they are completely amorphous. The pattern for the sample pyrolyzed at 1250°C shows a weak diffraction peak, suggesting the beginning of crystallization at this temperature. The intensity of the diffraction peak(s) increases with a further increase in the pyrolysis temperature, suggesting an increase in the crystallization degree. The weak diffraction peaks suggest that the samples are not completely crystallized up to 1400°C. All peak(s) can be identified as the βSiC phase.

The materials obtained were then analyzed using Raman spectroscopy, which is one of the most sensitive methods for the characterization of the different modifications of carbon.[14–17] The Raman spectrum recorded from the sample obtained at 1000°C shows no signals, suggesting that free carbon domains were not formed in this material. However, the elemental analysis suggested that there is extra carbon within the material (Table I). It is likely that the extra carbon has not formed a free carbon nanodomain yet at this pyrolysis temperature. Figure 3(a) shows a typical Raman spectrum of the sample pyrolyzed at 1200°C. The spectrum exhibits two bands at 1350 and 1600 cm^{-1}, which correspond to the D and G bands of the free carbon phase, suggesting that the extra carbon formed free carbon clusters at these higher temperatures.

The Raman spectra were used to calculate the size according to the following equation[18]:

$$L_a(nm) = (2.4 \times 10^{-10})\lambda_l^4 \left(\frac{I_D}{I_G}\right)^{-1} \quad (1)$$

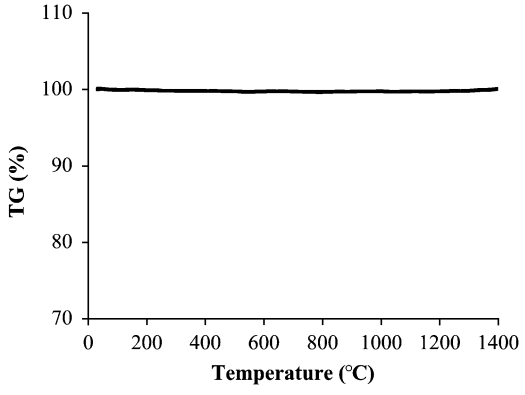

Fig. 1. TGA curve for the SiOC pyrolyzed at 900°C.

where I_D and I_G are the integrated intensities (areas) of the D and G bands, respectively; λ_l is the laser line wavelength (532 nm in the present study); and L_a is the domain size of the free carbon clusters. The results are summarized in Fig. 3(b). It is interesting to note that there is a critical temperature range between 1200° and 1300°C: below this range, the size of the free carbon first decreases with increasing pyrolysis temperature, while above this range, the free carbon size increases with increasing pyrolysis temperature. Note that the critical temperature range coincides with the crystallization starting temperature.

The point defects within the materials were analyzed using EPR. Figure 4(a) shows the room-temperature EPR spectrum of the samples obtained at 1200°C, measured at a frequency of 406.4 Hz. The spectrum consists of a symmetric line with a g value of 2.0032 ± 0.0002. This value suggests that the observed EPR line is due to the carbon dangling bonds (unpaired electrons) within the bulk SiC matrices, instead of within the free carbon clusters.[19] Figure 4(b) plots the peak-to-peak line width (reversely proportional to dangling bond concentration) of the EPR signal versus pyrolysis temperature. Again, a critical temperature range between 1200° and 1300°C is observed: below this, the line width decreases with increasing pyrolysis temperature, while above it, the line width increases with increasing pyrolysis temperature. This critical temperature range also coincides with the crystallization starting temperature.

The optical absorption behavior of these materials was measured to study their optical properties. According to Davis and Mott,[20] absorbance of an amorphous semiconductor as a function of photon energy $h\nu$ at higher photon energy regions follows:

$$(\alpha h\nu)^r \propto (h\nu - E_g). \quad (2)$$

where α is the absorbance of amorphous materials, E_g is the optical energy gap, and r is an index that characterizes the optical absorption process and may be 1/3, 1/2, 2/3, 1, and 2 depending on the transition mechanism in K space. Figure 5(a)

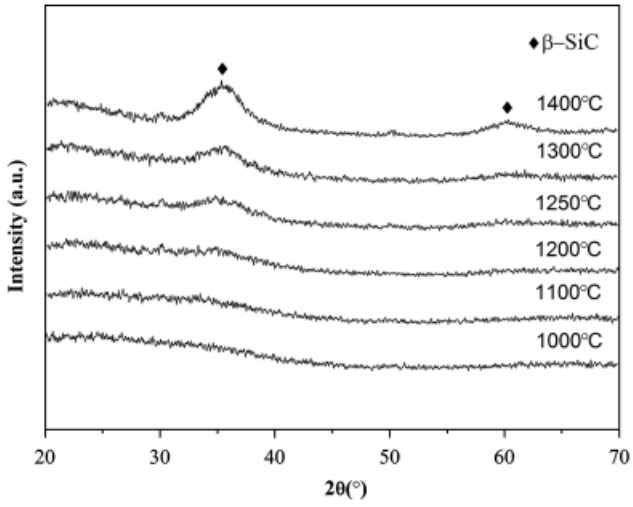

Fig. 2. XRD patterns for polymer-derived SiC pyrolyzed at different temperatures.

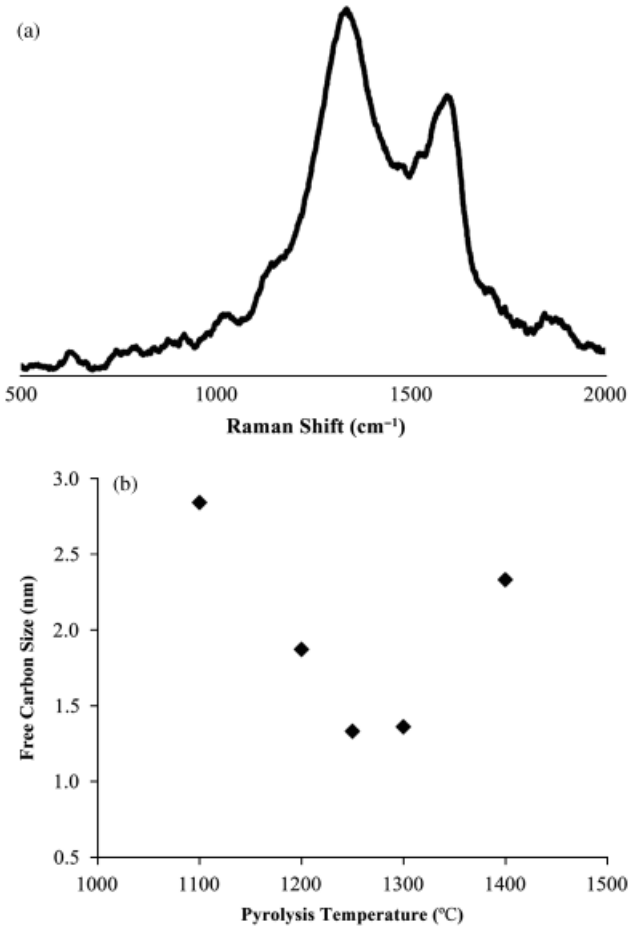

Fig. 3. (a) A typical Raman spectrum obtained from the SiC pyrolyzed at 1200°C. (b) The size of the free carbon phase as a function of pyrolysis temperature.

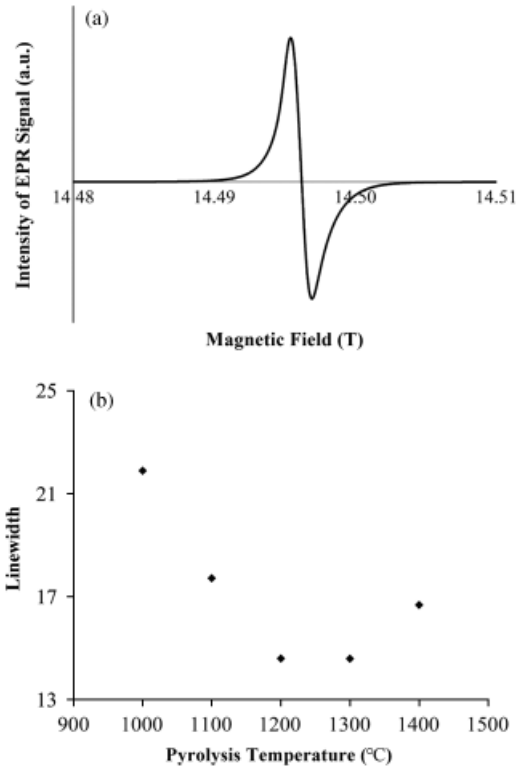

Fig. 4. (a) A typical EPR spectrum obtained from the SiC pyrolyzed at 1200°C. (b) The line width of the EPR signal as a function of pyrolysis temperature.

plots the $(\alpha h\nu)^2$ as a function of $h\nu$ for the materials obtained at 1100° and 1400°C. The linear relationship obtained at higher photon energy regions suggests that the absorptions are due to the transition between the two delocalized bands.[21–23] All amorphous SiOC obtained at different temperatures show similar behavior. The band gaps of these SiOCs are then estimated by extrapolation (indicated by the dotted lines in Fig. 5(a)) and summarized in Table II and Fig. 5(b) as a function of pyrolysis temperature. It can be seen that the band gaps of the SiOCs increase slowly with increasing pyrolysis temperature in temperature ranges between 100°–1100°C and 1300°–1400°C, but there is a relatively sharp increase in the band gap between 1200° and 1300°C. This temperature range also coincides with the critical temperature observed for structural changes.

Carefully examination of Fig. 5(a) reveals that the optical absorbance of the SiOCs is not zero at the lower excitation energy end, suggesting that there should be other absorption mechanisms at the lower excitation energy range. Tauc and colleagues[24–26] suggested that for amorphous semiconductors, the optical absorption spectra at a lower excitation energy range should follow

$$\alpha h\nu = B(h\nu - E_T)^n \tag{3}$$

This absorption was attributed to the transition from localized states (defect states) to delocalized states (conduction/valence band). The n can either be 1.5 or 0.5, depending on the distribution of these states.[24,26,27] E_T is an energy gap and B is a constant. According to Inkson,[28] for a nonallowed nonvertical transition from a deep impurity trap to a delocalized band, the n should be 1.5. Pfost *et al.*[27] further suggested that when n is around 1.5, E_T can be related to the electronic structures of amorphous semiconductors,

$$E_T = E_c - E_d \tag{4}$$

where E_c is the edge of an extended conduction band (also called the mobility edge) and E_d is a deep defect level with a high density of state.

In order to check whether there is a transition between the localized defect energy level and the delocalized bands in the materials, the absorption behavior of the SiOCs was measured in the low excitation energy range of 0.5–1.75 eV. The data were then analyzed using Eq. (3). It could be found that the spectra within this excitation range fitted the equation (Fig. 6). The n and E_d values obtained from curve fitting are summarized in Table II. Again, we see a clear transition around a pyrolysis temperature of 1200°–1300°C. At the lower pyrolysis temperature range, the n value obtained is closer to 1.5 as predicted by Eq. (3); thus, the absorption of the SiOCs is due to the transition between deep defect states and mobility edge. The defect level, E_d, for these materials is estimated and listed in Table II too. It can be seen that the E_d level increases with increasing pyrolysis temperature. On the other hand, at the higher pyrolysis temperature range, the n value significantly deviates from 1.5; thus, the absorption of these SiOCs over the lower excitation energy range cannot be explained by the transition between deep defect states and mobility edge. The transition mechanism for those materials pyrolyzed at higher temperatures is not clear to these authors, possibly related to the crystallized and/or high ordered structures of the materials.

IV. Discussion

The results observed on the structural changes (Figs. 2–4) are rather interesting. In particular, it seems that the change in the structures follows different trends below and above the critical temperature range, which consists of the crystallization initial

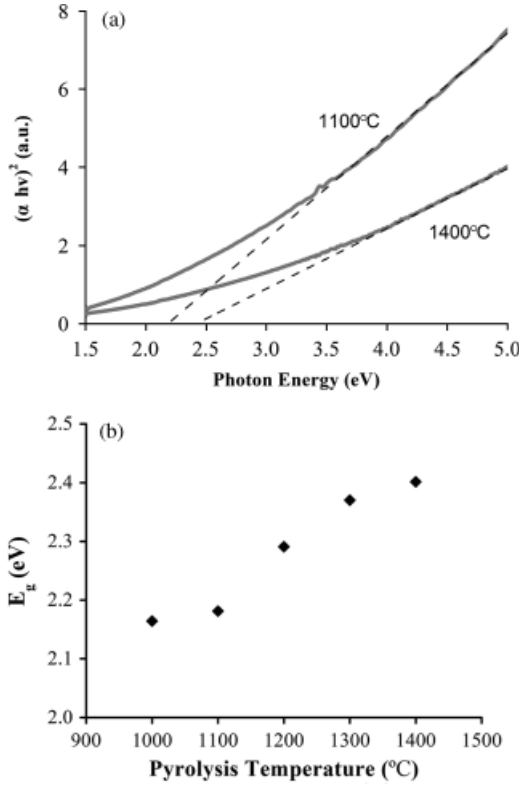

Fig. 5. (a) Plots of $(\alpha h\nu)^2$ as a function of photon energy for the SiC obtained at 1100° and 1400°C. (b) E_g as a function of pyrolysis temperature.

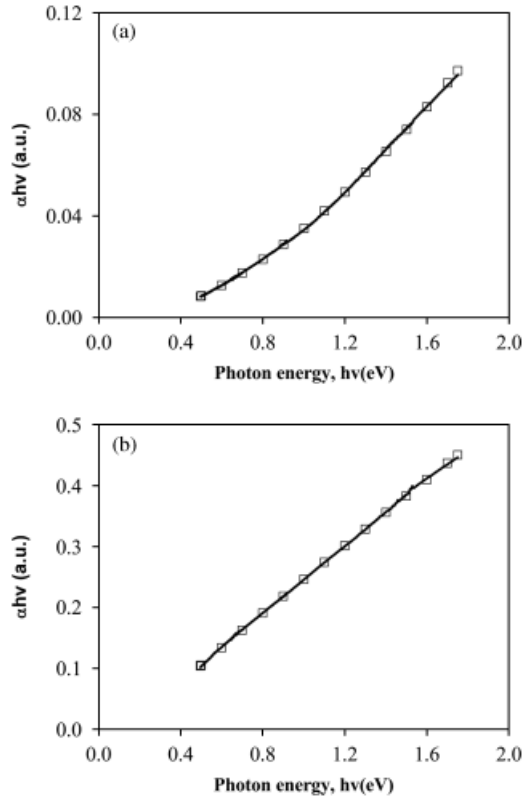

Fig. 6. Typical plots of $\alpha h\nu$ as a function of photon energy for the SiC materials pyrolyzed at (a) 1000°C and (b) 1300°C.

temperature range. Below the range, the size of the free carbon cluster decreases, while the concentration of the C-dangling bond within the SiOC matrix increases with increasing pyrolysis temperature. As the total amount of carbon remains the same for all the samples pyrolyzed at different temperatures (Table I), the above results suggest that carbon in free carbon clusters was dissolved in the amorphous matrix to form more Si–C bonds with increasing pyrolysis temperature, which leads to a higher C-to-Si ratio within the matrix. This indicates that the free carbon clusters formed before the critical temperature range are not stable, and carbon atoms prefer to remain in the more open structure of the amorphous matrix. On the other hand, above the critical temperature range, the size of the free carbon cluster increases and the concentration of the C-dangling bond decreases with increasing pyrolysis temperature; meanwhile, the amorphous SiOC phase starts to crystallize. This can be explained by the fact that when the amorphous SiOC phase starts to crystallize, the C-to-Si ratio within the matrix phase decreases and tends toward 1:1. As a consequence, the extra carbon atoms within the matrix are expelled and deposited on the surface of the free carbon clusters, leading to an increase in free carbon size and decreases in C-dangling bonds.

The change in the optical absorption band gap can be attributed to structural changes. Previous studies on amorphous silicon carbide prepared by chemical vapor deposition revealed that E_g increases with increasing C/Si ratio due to the replacement of weaker Si–Si bonds by stronger Si–C bonds.[29–31] This was consistent with the current results obtained for the materials pyrolyzed at lower temperatures. For these materials, the concentration of the C-dangling bond increases with increasing pyrolysis temperature, resulting in an increase in the C/Si ratio within the amorphous SiOC matrix and an increase in band gap. For the materials pyrolyzed at higher temperatures, the SiOC matrix phase has a much higher degree of order (as can be seen from the start of crystallization) and the degree of order increases with increasing pyrolysis temperature. The materials behave more like a crystalline counterpart, which has a much higher E_g value.

It can be seen from Table II that E_d is a function of line width of EPR signal. The result reveals that the E_d increases with increasing concentration of the C-dangling bonds. Similar results have also been obtained by previous studies,[11,32] which reported that E_d within polymer-derived amorphous SiOCN was associated with carbon dangling bands. This phenomenon can be explained by considering dangling bands that have unpaired electrons as defects and generate a deep defect level within the band gap. This defect level expands with an increase in the defect concentration.

Table II. Curve Fitting Parameters for the Amorphous Silicon Carbides

Sample #	Pyrolysis temperature (°C)	E_g (eV)	n	E_d (eV)
S1	1000	2.16	1.61	2.02
S2	1100	2.18	1.40	2.07
S3	1200	2.29	1.24	2.14
S5	1300	2.37	0.95	/
S6	1400	2.40	1.14	/

V. Summary

In this paper, the structure and optical behavior of polymer-derived SiOC ceramics pyrolyzed at different temperatures are studied. We find that below a temperature range of 1200°–1300°C, the size free carbon cluster decreases and the C-dangling bond increases with pyrolysis temperature, suggesting that the C within the free carbon phase was dissolved in the matrix phase with increasing pyrolysis temperature, while above this temperature range, the size free carbon cluster increases and the C-dangling bond decreases with pyrolysis temperature, suggesting that the C within the matrix phase was precipitated on the free

carbon phase. Meanwhile, the material starts to crystallize within this temperature range. We also find that the optical behavior of the materials is different below and above this critical temperature range. Below the temperature range, both structure and optical behavior of the materials act more like an amorphous material, while above the range, they act more like a crystal and/or highly ordered materials.

References

[1]E. Kroke, Y. L. Li, C. Konetschny, E. Lecomte, C. Fasel, and R. Riedel, "Silazane Derived Ceramics and Related Materials," *Mater. Sci. Eng.*, **R26**, 97–199 (2000).

[2]A. Saha, R. Raj, and D. L. Williamson, "A Model for the Nanodomains in Polymer-Derived SiCO," *J. Am. Ceram. Soc.*, **89**, 2188–98 (2006).

[3]S. Traßl, D. Suttor, G. Motz, E. Rössler, and G. Ziegler, "Structural Characterization of Silicon Carbonitride Ceramics Derived from Polymeric Precursors," *J. Eur. Ceram. Soc.*, **20**, 215–25 (2000).

[4]P. Colombo, G. Mera, R. Riedel, and G. D. Sorarù, "Polymer-Derived Ceramics: 40 Years of Research and Innovation in Advanced Ceramics," *J. Am. Ceram. Soc.*, **93** [7] 1805–37 (2010).

[5]Y. Wang, W. Fei, Y. Fan, L. Zhang, W. Zhang, and L. An, "A Silicoaluminum Carbonitride Ceramic Resist Oxidation/Corrosion in Water Vapor," *J. Mater. Res.*, **21** [7] 1625–8 (2006).

[6]C. Haluschka, C. Engel, and R. Riedel, "Silicon Carbonitride Ceramics Derived From Polysilazanes Part II. Investigation of Electrical Properties," *J. Euro. Ceram. Soc.*, **20**, 1365–74 (2000).

[7]P. A. Ramakrishnan, Y. Wang, D. Balzar, L. An, C. Haluschka, R. Riedel, and A. M. Hermann, "Silicoboron-Carbonitride Ceramics: A Class of High-Temperature, Dopable Electronic Materials," *Appl. Phys. Lett.*, **78**, 3076–8 (2001).

[8]Y. Wang, L. Zhang, W. Xu, T. Jiang, Y. Fan, D. Jiang, and L. An, "Effect of Thermal Initiator Concentration on the Electrical Behavior of Polymer-Derived Amorphous Silicon Carbonitrides," *J. Am. Ceram. Soc.*, **91** [12] 3971–5 (2008).

[9]Y. Wang, T. Jiang, L. Zhang, and L. An, "Electron Transport in Polymer-Derived Amorphous Silicon Oxycarbonitride Ceramics," *J. Am. Ceram. Soc.*, **92** [7] 1603–6 (2009).

[10]L. Zhang, Y. Wang, Y. Wei, W. Xu, D. Fang, L. Zhai, K. Lin, and L. An, "Asilicon Carbonitride Ceramic with Anomalously High Piezoresistivity," *J. Am. Ceram. Soc.*, **91** [4] 1346–9 (2008).

[11]Y. Wang, T. Jiang, L. Zhang, and L. An, "Optical Absorption in Polymer-Derived Amorphous Silicon Oxycarbonitrides," *J. Am. Ceram. Soc.*, **92** [12] 3111–3 (2009).

[12]L. Ferraioli, D. Ahn, A. Saha, L. Pavesi, and R. Raj, "Intensely Photoluminescent Pseudo-Amorphous Silicon Oxycarbonitride Polymer-Ceramic Hybrides," *J. Am. Ceram. Soc.*, **91**, 2422–4 (2008).

[13]Y. Wang, J. Ding, W. feng, and L. An, "Effect of Pyrolysis Temperature on the Piezoresistivity of Polymer-Derived Ceramics," *J Am. Ceram. Soc.*, **94** [2] 359–62 (2011).

[14]Y. Wang, D. C. Alsmeyer, and R. L. McCreery, "Raman Spectroscopy of Carbon Materials: Structural Basis of Observed Spectra," *Chem. Mater.*, **2**, 557–63 (1990).

[15]M. I. Nathan, J. E. Jr. Smith, and K. N. Tu, "Raman Spectra of Glassy Carbon," *J. Appl. Phys.*, **45**, 2370 (1974).

[16]F. Tuinstra and J. L. Koenig, "Raman Spectrum of Graphite," *J. Chem. Phys.*, **53** [3] 1126–30 (1970).

[17]L. C. Nistor, J. Van Landuyt, V. G. Ralchenko, T. V. Kononenko, E. D. Obraztsova, and V. E. Strelnitsky, "Direct Observation of Laser-Induced Crystallization of a-C:H Films," *Appl. Phys. A*, **58**, 137–44 (1994).

[18]L. G. Cançado, K. Takai, and T. Enoki, "General Equation for the Determination of the Crystallite Size La of Nanographite by Raman Spectroscopy," *Appl. Phys. Lett.*, **88**, 163106 (2006).

[19]E. Tomasella, M. Dubois, C. Meunier, and L. Thomas, "Characterization by Electron Spin Resonance of Defects in a-C:H Thin Films. Correlation Between Structural Evolutions and Optical Properties," *Surf. Coat. Technol.*, **180–181**, 227–33 (2004).

[20]E. A. Davis and N. F. Mott, "Conduction in Non-Crystalline Systems: Conductivity, Optical Absorption and Photoconductivity in Amorphous Semiconductors," *Phil. Mag.*, **22**, 903–22 (1970).

[21]S. V. Deshpande, E. Gulari, S. W. Brown, and S. C. Rand, "Optical Properties of Silicon Nitride Films Deposited by Hot Filament Chemical Vapor Deposition," *J. Appl. Phys.*, **77**, 6534–41 (1995).

[22]J. H. Simmons and K. S. Potter, *Optical Materials*. Academic Press, London, 2000.

[23]S. T. Kshirsagar and A. P. B. Sinha, "Optical Absorption, Electrical Conductivity and Spectral Response Measurements on the System CdGaSSe," *J. Mater. Sci.*, **12**, 1614–24 (1977).

[24]S. I. Andronenko, I. Stiharu, and S. K. Misra, "Synthesis and Characterization of Polyureasilazane Derived SiCN Ceramics," *J. Appl. Phys.*, **99**, 113907 (2006).

[25]P. O'Connor and J. Tauc, "Photoinduced Midgap Absorption in Tetrahedrally Bonded Amorphous Semiconductors," *Phys. Rev. B*, **25**, 2748–66 (1982).

[26]P. O'Connor and J. Tauc, "Spectrum of Photoinduced Optical Absorption in a-Si:H," *Solid State Commun.*, **36**, 947–9 (1980).

[27]D. Pfost, H. Liu, Z. Vardeny, and J. Tauc, "Photo-Induced Absorption Spectra in Ge:H and Si:H," *Phys. Rev. B*, **30**, 1083–6 (1984).

[28]J. C. Inkson, "Deep Impurities in Semiconductors: 11. The Optical Cross Section," *J. Phys. C: Solid State Phys.*, **14**, 1093–101 (1981).

[29]A. Desalvo, F. Giorgis, C. F. Pirri, E. Tresso, P. Rava, R. Galloni, R. Rizzoli, and C. Summpnte, "Optoelectronic Properties, Structure and Composition of α-SiC:H Films Grown in Undiluted and H2 Diluted Silane-Methane Plasma," *J. Appl. Phys.*, **81**, 7973–80 (1997).

[30]K. Mui, D. K. Basa, F. W. Smith, and R. Corderman, "Optical Constants of A Series of Amorphous Hydrogenated Silicon-Carbon Alloy Films: Dependence of Optical Response on Film Microstructure and Evidence for Homogeneous Chemical Ordering," *Phys. Rev. B*, **35**, 8089–102 (1987).

[31]J. Robertson, "The Electronic and Atomic Structure of Hydrogenated Amorphous Si–C Alloys," *Philos. Mag. B*, **66**, 615–38 (1992).

[32]S. Trassl, G. Motz, E. Rossler, and G. Ziegler, "Characterization of Free Carbon Phase in Precursor Derived SiCN Ceramics: q, Spectroscopic Methods," *J. Am. Ceram. Soc.*, **85**, 239–44 (2002). □